*Published online 29 January 2013*

*Nucleic Acids Research, 2013, Vol. 41, No. 7* ***e80***
*doi:10.1093/nar/gkt031*

# Efficient self-assembly of DNA-functionalized fluorophores and gold nanoparticles with DNA functionalized silicon surfaces: the effect of oligomer spacers

**James A. Milton[1], Samson Patole[2], Huabing Yin[2], Qiang Xiao[3], Tom Brown[3] and Tracy Melvin[2,4,*]**

[1]National Oceanography Centre, University of Southampton, Southampton, Hampshire, SO14 3ZH, [2]School of Electronics and Computer Science, University of Southampton, Southampton, Hampshire, SO17 1BJ, [3]School of Chemistry, University of Southampton, Southampton, Hampshire, SO17 1BJ and [4]Optoelectronics Research Centre, University of Southampton, Southampton SO17 1BJ, Hampshire, UK

Received October 15, 2012; Revised December 5, 2012; Accepted January 4, 2013

## ABSTRACT

**Although strategies for the immobilization of DNA oligonucleotides onto surfaces for bioanalytical and top-down bio-inspired nanobiofabrication approaches are well developed, the effect of introducing spacer molecules between the surface and the DNA oligonucleotide for the hybridization of nanoparticle–DNA conjugates has not been previously assessed in a quantitative manner. The hybridization efficiency of DNA oligonucleotides end-labelled with gold nanoparticles (1.4 or 10 nm diameter) with DNA sequences conjugated to silicon surfaces via hexaethylene glycol phosphate diester oligomer spacers (0, 1, 2, 6 oligomers) was found to be independent of spacer length. To quantify both the density of DNA strands attached to the surfaces and hybridization with the surface-attached DNA, new methodologies have been developed. Firstly, a simple approach based on fluorescence has been developed for determination of the immobilization density of DNA oligonucleotides. Secondly, an approach using mass spectrometry has been created to establish (i) the mean number of DNA oligonucleotides attached to the gold nanoparticles and (ii) the hybridization density of nanoparticle–oligonucleotide conjugates with the silicon surface–attached complementary sequence. These methods and results will be useful for application with nanosensors, the self-assembly of nanoelectronic devices and the attachment of nanoparticles to biomolecules for single-molecule biophysical studies.**

## INTRODUCTION

Silicon is used ubiquitously by the semiconductor industry, and nanofabrication approaches have been both implemented and are being developed for ever smaller devices. The uniform chemical reactivity of crystalline silicon makes it an ideal substrate for the direct immobilization of biomolecules, so permitting the use of silicon structures for biosensors and for the self-assembly DNA/nanomaterial conjugates as building blocks in the creation of nanostructures by the so-called 'bottom-up' methods for the next generation of nanoelectronic devices. During the past decade, a number of approaches have been developed for the covalent attachment of DNA oligonucleotides onto crystalline silicon surfaces (1–5), and sub-micron motifs of surface-attached DNA oligonucleotides in high densities on silicon can be achieved (5). Although approaches for the creation of hybrids of DNA-conjugated nanosized particles to surface-attached DNA has been reported (6,7), there has not been a systematic study of the hybridization efficiency of DNA oligonucleotide–nanoparticle conjugates, and this information is crucial for the creation of next-generation nanobiosensors and bio-inspired self-assembly of nanoelectronic devices. This is especially important for the so-called 'bottom-up'–based nanofabrication methods (8,9).

*To whom correspondence should be addressed. Tel: +44 2380 596505; Fax: +44 2380 593149; Email: tm@ecs.soton.ac.uk
Present address:
Huabing Yin, School of Engineering, James Watt South Building, University of Glasgow, Glasgow G12 9QQ, UK.

The authors wish it to be known that, in their opinion, the first three authors should be regarded as joint First Authors.

In comparison with the case of solution-phase DNA hybridization, the requirements for effective DNA hybridization to conjugated DNA sequences on surfaces is not so well understood. It has been shown that the density of immobilized DNA, or probe, on a substrate strongly affects the hybridization yield of unlabelled or fluorophore-labelled DNA as well as the kinetics of hybridization such that high efficiency of hybridization is usually achieved in low-density regimes (10–12). Although low densities may be preferable for some bioanalysis applications, where the size of the sensor or device surface area reaches the nanoscale, then the number of conjugated DNA strands is limited by the size and sometimes infinitesimally small. So for nanoscale sensors and devices, understanding the conditions for achieving high hybridization efficiencies and densities of DNA conjugates to complementary DNA strand surfaces is important.

The steric hindrance, the accessibility and surface charge of surface-immobilized DNA probe as well as the ionic strength towards hybridization with an unlabelled or fluorophore-labelled complementary sequence has been the subject of a number of studies (10,11,13–20). The most common approach to improve the hybridization efficiency of complementary strands with surface-attached DNA probe sequences involves the use of 'spacers', which are conjugated between the surface and the probe (21). These spacers have a number of effects including (i) 'raising' the DNA probe from the surface (ii) impacting on the local electrostatic and hydrophilic environment of the DNA probe, (iii) influencing the 'steric' accessibility of the DNA probe to hybridization and (iv) producing 'brush-like' surfaces (10,11,13–15,22). In addition, some spacer molecules, for instance oligomers of ethylene glycol, can reduce non-specific association of DNA complementary sequences with the surface (16,17).

Spacers that are based on oligomers of ethylene glycol are considered to facilitate the hybridization of fluorophore-labelled or unlabelled DNA oligonucleotides with surface-attached complementary sequences (16,17,23,24). Perhaps the most well-known study in this field is that of Southern *et al.* (17), where the effect of surface density of the attached sites and of ethylene glycol oligomers with different lengths and containing different charged groups has been investigated. These studies suggest that the optimal spacer is one with a low negative-charge density that is amphiphilic and has a chain length of 30–60 atoms. Longer or shorter spacers were found to be detrimental to the hybridization yield with oligonucleotides. More recently, Peeters *et al.* have investigated the effect of hexyl and undecyl alkane spacers linked to a gold surface and then linked via triethylene glycol and hexaethylene glycol phosphate diester groups to DNA oligonucleotides (25). It is proposed that the use of the undecyl groups provides DNA films in which the molecules are oriented perpendicular to the surface. Unfortunately no conclusions could be deduced regarding the effect of ethylene glycol oligomer size on the hybridization efficiency from that study.

Rather than synthesize oligonucleotides and linkers directly on surfaces as reported by Southern *et al.* (17), the approach taken here is to first attach a monolayer of *N*-succinimide ester functionalized undecyl alkane chains on the surface in a similar approach to Peeters *et al.* (25) and then conjugate these to DNA oligonucleotides with a 'spacer' of hexaethylene glycol phosphate diester oligomers between the DNA 3′-end and a hexylamine linker for reaction with the succinimide group at the surface. This strategy was used to provide both a high and the same immobilized density of DNA conjugated to the surface (irrespective of the spacer length).

The density for hybridization of DNA to silicon surfaces (without a spacer) has previously been established by us to be $7 \times 10^{12}$ DNA oligonucleotides per square centimetre (5). This is slightly higher than for covalently attached DNA on glass surfaces ($2.3 \times 10^{12}$ DNA oligonucleotides per square centimetre) (2). The presence of oligomers of hexaethylene glycol phosphate diester spacers between the oligonucleotide and the linker on the surface is anticipated to facilitate the hybridization of DNA oligonucleotides conjugated to gold nanoparticles (DNA–GNP). Using relatively high densities of immobilized DNA sequences on the surface is anticipated to reduce the probability of the DNA sequences being positioned within the surface-immobilized ethylene glycol oligomers at the surface (21,22), and thus allow access of the bulky GNP–DNA (26,27).

The impact of spacers on the conjugation efficiency and hybridization of DNA to DNA–GNP has been the subject of a number of studies (9,27–30), It is the disassembly of DNA–GNPs with complementary DNA–GNPs that has provided the most interest, where cooperative thermal denaturation or enzymatic cleavage result in a colour change (31,32). The kinetics for the assembly of DNA–GNP with complementary DNA–GNP is often slow and has been the subject of a number of recent studies (33–35), notably Oh *et al.*, who demonstrated that the use of spacers of polynucleotides of adenine or thymine between the oligonucleotide and the GNP impacts on the hybridization kinetics; a spacer of 15 nucleotides was considered optimal, and additional nucleotides in the space did not improve the hybridization rate (35). Given the wealth of literature for the assembly of DNA–GNP with complementary DNA–GNPs, there are few examples of nanoparticles conjugated to oligonucleotides that have been hybridized with oligonucleotides attached to planar surfaces (6,7,36); optimized conjugation for highly efficient assembly has not been studied in detail before now.

In this article, we investigate the influence of the oligomer spacer length on the hybridization performance of immobilized DNA. To achieve this, we have developed novel methods to quantitatively assess the density of (i) immobilized DNA oligonucleotide probes on the silicon surface, (ii) DNA oligonucleotides attached to GNPs and (iii) hybridized targets, including DNA–GNP conjugates.

## MATERIALS AND METHODS

### Reagents

All chemicals were obtained from the Aldrich Chemical Company unless otherwise noted and used without further

**Table 1.** DNA oligonucleotide sequences

| Reference | Sequence[a] |
|---|---|
| A-HEG$_0$ | 3′-NH$_2$-(CH$_2$)$_4$CH(CH$_2$OH)CH$_2$-TGA CGA TAG ATA GAC GT-5′ |
| A-HEG$_1$ | 3′-NH$_2$-(CH$_2$)$_4$CH(CH$_2$OH)CH$_2$-(HEG)$_1$-TGA CGA TAG ATA GAC GT-5′ |
| A-HEG$_2$ | 3′-NH$_2$-(CH$_2$)$_4$CH(CH$_2$OH)CH$_2$-(HEG)$_2$-TGA CGA TAG ATA GAC GT-5′ |
| A-HEG$_6$ | 3′-NH$_2$-(CH$_2$)$_4$CH(CH$_2$OH)CH$_2$-(HEG)$_6$-TGA CGA TAG ATA GAC GT-5′ |
| A-EG$_{91}$ | 3′-NH$_2$-(CH$_2$)$_4$CH(CH$_2$OH)CH$_2$-PEG4000-TGA CGA TAG ATA GAC GT-5′ |
| B-HEG$_0$ | 3′-NH$_2$-(CH$_2$)$_4$CH(CH$_2$OH)CH$_2$-TGA CGA TAG ATA GAC GT***P***T-FAM-5′ |
| B-HEG$_1$ | 3′-NH$_2$-(CH$_2$)$_4$CH(CH$_2$OH)CH$_2$-(HEG)$_1$-TGA CGA TAG ATA GAC GT***P***T-FAM-5′ |
| B-HEG$_2$ | 3′-NH$_2$-(CH$_2$)$_4$CH(CH$_2$OH)CH$_2$-(HEG)$_2$-TGA CGA TAG ATA GAC GT***P***T-FAM-5′ |
| B-HEG$_6$ | 3′-NH$_2$-(CH$_2$)$_4$CH(CH$_2$OH)CH$_2$-(HEG)$_6$-TGA CGA TAG ATA GAC GT***P***T-FAM-5′ |
| A′-com | 3′-ACG TCT ATC TAT CGT C-FAM-5′ |
| A′1-mis | 3′-ACG TCT ATC T***T***T CGT C-FAM-5′ |
| A′-non | 3′-CTT ATG CTA GCC ATT C-FAM-5′ |
| C-com | 3′-FAM-ACG TCT ATC TAT CGT C-5′ |
| D-HEG$_0$ | 3′-NH$_2$-(CH$_2$)$_4$CH(CH$_2$OH)CH$_2$-ACG TCT ATC TAT CGT C-5′ |
| E-HEG$_0$ | 3′-HS-(CH$_2$)$_6$-ACG TCT ATC TAT CGT C-5′ |
| E-HEG$_6$ | 3′-HS-(CH$_2$)$_6$-(HEG)$_6$-ACG TCT ATC TAT CGT C-5′ |

[a]HEG, hexaethylene glycol diphosphate ester; ***P***, photolabile linker; ***T***, mismatch nucleotide.

purification. Deionized (DI) water (ELGA genetics system) was used for the preparation of all the aqueous solutions. Undecylenic acid *N*-hydroxysuccinimide ester (UANHS) was synthesized as described elsewhere (4). The oligonucleotides used for this study (Table 1) were synthesized in-house using conventional phosphoramidite chemistry and purified by reverse-phase high pressure (or high performance) liquid chromatography (HPLC). The A-series oligonucleotides for attachment to the UANHS linker functionalized silicon surface were synthesized with an aminomodifier C7 CpG (Glen Research) at the 3′-end, and hexaethylene glycol diphosphate ester (HEG) spacers were synthesized by inserting one, two or six 17-O-(4,4′-dimethoxytrityl)-hexaethyleneglycol, 1-[(2-cyanoethyl)-(*N*,*N*-diisopropyl)]-phosphoramidite units (Link Technologies) and oligonucleotides with 92 ethylene glycol oligomers by addition of the PEG4000 NHS ester (Creative PEGWorks) to the aminohexyl group on the 3′-end of the oligonucleotide [identical to A-(HEG)$_0$] following the solid-phase oligonucleotide synthesis. The B-series of oligonucletides prepared to establish the surface-attachment density were synthesized by incorporation of the photolabile group, 3-(4,4′-dimethoxytrityl)-1-(2-nitrophenyl)-propane-1,3-diol-[2-cyanoethyl-(*N*, *N*-diisopropyl)]-phosphoramidite (Link Technologies) between the DNA sequence and 6-carboxyfluorescein (FAM), which allowed the photolytic release of the fluorophore groups from the oligonucleotides on ultraviolet (UV) irradiation (37). For the preparation of DNA–GNP conjugates, 3′-aminomodified oligonucleotides (the D-series) and 3′-thiolmodified oligonucleotides (the E-series), all with a complementary sequence to the A-series, were synthesized.

### Photopatterning of silicon surfaces with undecylenic acid *N*-hydroxysuccinimide

Masks were prepared on UV-grade fused silica (Suprasil) by chrome evaporation followed by patterning by photolithography and removal of the revealed chrome areas using the wet etching method. This was followed by removal of the lithographic resist in acetone and thorough cleaning. Diced pieces ($2 \times 2$ cm$^2$) of single-side polished silicon <100> wafer were precleaned (RCA clean), etched in 2% hydrofluoric acid for 2 min, washed thoroughly with water, dried under pressurized nitrogen and immediately spin-coated with 40 µl of 1% UANHS solution in $CH_2Cl_2$ at 2000 r.p.m. for 50 s (4). The wafer was exposed through a quartz mask in contact (containing parallel lines of 10 µ wide with 30 µ spacing over a total area of 18 mm$^2$) under nitrogen protection using a 500-W HgXe lamp (Oriel Instrument) fitted with an interference filter (253.7 ± 10 nm, Melles Griot) at 1 mW/cm$^2$ for 5 min. After photoreaction, the wafer was thoroughly washed with dichloromethane.

### Immobilization of DNA oligonucleotides onto the succinimidyl ester functionalized silicon surface

The A-series of oligonucleotides used for immobilization were dissolved in a 0.1 M sodium bicarbonate solution to a final concentration of 50 µM (pH = 8.3). Eight micro litre of the oligonucleotide solution was deposited on the UANHS alkene-patterned silicon wafer and covered with a cover slip ($2 \times 2$ cm$^2$). The wafer was incubated overnight at room temperature in a humid chamber. After incubation, the wafer was washed thoroughly with DI water. Samples immobilized with the oligonucleotides were kept in DI water at 4°C before characterization or hybridization.

### Preparation of DNA oligonucleotide–gold nanoparticle conjugates

(i) Gold nanoparticles (1.4 nm diameter) with a single DNA oligonucleotide linked to the surface were prepared as follows: mono-*N*-succinimide functionalized 1.4 nm GNPs (Mono-sulfo-NHS-Nanogold, Nanoprobes) at a concentration of 15 µM in 10 mM sodium phosphate buffer at pH 8.0 were mixed with two equivalents of the D-series oligonucleotides at 4°C overnight, and then purified by ultracentrifugation (67 000*g*) and triple washing of the pellet with 10 mM phosphate buffer,

0.3 M NaCl, pH 7.0, to yield the 3′-GNP end-labelled DNA conjugate ($HEG_0$-GNP 1.4 nm).

(ii) Ten-nanometre diameter colloidal GNPs were conjugated with multiple DNA oligonucleotides per particle using a similar procedure to that previously reported (28). The E-series oligonucleotides were treated with 0.1 M dithiothreitol (DTT) in 0.1 M $NaHCO_3$ at room temperature for 1 h to activate the thiol terminal groups. After the extra DTT was extracted with ethyl acetate, the oligonucleotides were desalted using a Nap-10 column (Pharmacia) and freeze dried. The activated thiol oligonucleotides were incubated with 10 nm diameter GNPs (BBInternational) at 4°C overnight typically in a ratio of 0.009 μmole gold nanoparticles to 1.8 μmole oligonucleotides. The DNA–GNP (10 nm diameter) conjugates were gradually exposed to 10 mM phosphate buffer, 0.1 M NaCl, pH 7.0 for 16 h for 'aging', and then purified by ultracentrifugation (26 000*g*) and triple washing of the pellet with 10 mM phosphate buffer, 0.1 M NaCl, pH 7.0. The final product was re-suspended and stored in a 10 mM phosphate buffer, 0.3 M NaCl, pH 7.0 solution. The concentration of the final DNA–GNP concentrations was estimated by UV-visible spectroscopy. The extinction coefficients of the characteristic adsorption peaks of gold nanoparticles [420 nm for 1.4 nm (Nanoprobe Inc.) and 520 nm for 10 nm gold particles] did not change significantly as a result of the oligonucleotide attachment (28).

### Hybridization and denaturation of fluorophore and gold nanoparticle DNA conjugates from surface-attached DNA

FAM-labelled A′-series or C-series oligonucleotides (20 μM) were dissolved in phosphate-buffered saline (10 mM phosphate buffer, 0.3 M NaCl, pH 7.0) for hybridization. A wafer patterned with an A-series oligonucleotide was pre-soaked in phosphate-buffered saline for 20 min, and then excess buffer was removed. Immediately afterwards, 8 μl of the oligonucleotide hybridization solution was deposited on the wafer and covered with a cover slip. The wafer was incubated in a humid chamber for 4 h at room temperature. After incubation, the wafer was rinsed thoroughly and then stored in the phosphate buffer.

The GNP conjugates (either 1.4 or 10 nm) with D-series or E-series oligonucleotides (~10 nM) were dissolved in phosphate-buffered saline (10 mM phosphate buffer, 0.3 M NaCl, pH 7.0) for hybridization. A pre-soaked wafer patterned with an A-series oligonucleotide was treated with 20 μl of the oligonucleotide–GNP hybridization solution and incubated in a humid chamber for 8 h at room temperature. After incubation, the wafer was rinsed thoroughly and then stored in the phosphate buffer.

### Quantification of the surface-immobilization density and hybridization efficiency

#### *Surface-immobilization density*

Photolysis conditions for cleaving the photolabile group from the surface-attached B-series oligonucleotides were optimized. Typically, the sample dissolved in DI water was illuminated through a band pass filter (345~395 nm) with a 500-W HgXe lamp at various intensities and exposure times. The photolysis products were analysed by HPLC to determine the percentage of oligonucleotide chains cleaved from the FAM group in comparison with the starting intact oligonucleotide (i.e. the photolysis yield). The optimum conditions were found to be 30-min illumination at 25–30 mW/cm$^2$. The B-series of oligonucleotides were attached to the silicon surface in patterns by the same method used for the A-series oligonucleotide attachment and described above. The wafer with the B-series oligonucleotide patterns was photolysed using the optimal conditions determined above, and then placed in 800 μl of water at 90°C for 15 min to dissolve the cleaved FAM groups. The wafer was removed, rinsed twice with 100 μl water and evaluated by fluorescence microscopy to make sure all the fluorophores had been removed. The collected solution (1000 μl) was freeze dried. The resulting material was re-dissolved in 70 μl of 0.05 M Tris buffer (pH 8.7) and the fluorescence yield measured in a 50 μl cuvette by fluorimeter (Cary Ellipse, Varian Inc., $\lambda_{exc}$ = 488 nm, $\lambda_{em}$ = 525 nm). The concentration of cleaved fluorophore groups present was determined by reference to a standardization curve produced by illumination [30 min illumination at 25–30 mW/cm$^2$ (345~395 nm)] of a series of solutions of known concentration of the oligonucleotides containing the photolabile and FAM groups in DI water.

#### *Hybridization density with single-stranded DNA*

The hybridization density was quantified using our previously reported method (5). Briefly, A-series oligonucleotides were patterned on silicon surfaces using a photolithographic mask. Complementary fluorescent oligonucleotides (C-com) were hybridized on to the A-series oligonucleotide patterns and washed thoroughly with phosphate buffer. Fluorescent images were acquired to confirm hybridization and calculate the surface area of the oligonucleotide patterns. The wafer was then placed in 800 μl of water at 90°C for 15 min to allow for the denaturation of the duplex. The wafer was removed and rinsed twice with 200 μl of water and the wash collected. The wafer was examined by fluorescence microscopy to make sure all the C-com had been removed. The water was removed in a freeze drier and then the residue carefully dissolved in 70 μl of 0.05 M Tris buffer (pH 8.7). The fluorescence yield from the sample was measured in a 50 μl cuvette in a fluorimeter (Cary Ellipse, Varian Inc., $\lambda_{exc}$ = 488 nm, $\lambda_{em}$ = 525 nm); at least four separate samples were determined. The concentration of DNA strands present in the sample was determined by reference to a standardization curve prepared from a series of fluorescent-labelled DNA oligonucleotide samples of known concentration.

#### *Quantification of DNA–gold nanoparticle conjugates hybridized to the DNA functionalized surfaces*

The conjugates hybridized on to A-series oligonucleotide patterns attached on the surface of the silicon were released by heating in water at 90°C for 15 min, and the collected DNA–GNP conjugate solutions were too dilute to establish the concentration by absorption spectroscopy,

so a mass spectrometry method was developed to establish the hybridization density, and this is achieved by measurement of the gold concentration following chemical digestion as follows: it is assumed that the density of spherical gold nanoparticles is equivalent to that of bulk gold ($=19.30\,g/cm^3$), so the average particle mass was calculated to be $2.77 \times 10^{-20}$ g for 1.4 nm gold and $1.01 \times 10^{-17}$ g for 10 nm gold nanoparticles. By establishing the mass of gold in a DNA–GNP conjugate solution as compared with the theoretical nanoparticle mass allows for the number of GNPs to be determined. The samples were prepared for inductively coupled plasma–mass spectroscopy (ICP–MS) analysis by digestion of the collected DNA–GNP conjugates in water (1 ml) with 50 µl of 0.1 M KCN and 1 mM $K_3Fe(CN)_6$ for 1 h to dissolve the gold nanoparticles. This solution was then diluted with 9 ml of 5% HCl and analysed by ICP–MS following the method described in Pitcairn *et al*. (38). Control samples prepared in the same manner without DNA–GNP but with similar amounts of oligonucleotides were used as background reference samples. All measurements were repeated four times.

### *Quantification of the number of oligonucleotides attached to the 10-nm diameter gold nanoparticles*

The surface coverage of DNA strands on 10-nm GNPs was determined using a combination of ICP–MS and inductively coupled plasma–optical emission spectroscopy (ICP–OES) methods. The number of DNA strands was calculated from the phosphorus concentration determined by ICP–OES using the following method. To avoid adventitious phosphate contamination, the DNA–GNP conjugates were aged in 0.1 N NaCl solution (pH ~7.0). 150 µl of the DNA–GNP conjugate solution was weighed and transferred to a polytetrafluoroethylene high-pressure microwave digestion vessel and then spiked with an yttrium as an internal standard. Following the addition of 1 ml of sub-boiled concentrated $HNO_3$, the DNA–GNP samples were digested for 30 min using a microwave digestor (CEM, MDS2000). The digested samples were transferred to polyethylene containers and then diluted with 10 ml ultrapure water. The concentration of phosphorus was determined using ICP–OES calibrated with synthetic reference standards. The number of moles of phosphorus was calculated from the determined mass divided by the atomic mass of phosphorus (30.9736). The number of moles of the target oligonucleotide was calculated by dividing the number of phosphate groups in the oligonucleotides ($E\text{-}HEG_0$) = 17 and ($E\text{-}HEG_6$) = 23.

The number of target DNA sequences attached per gold nanoparticle was established by the determination of the gold nanoparticle numbers in a comparable solution, but using the ICP–MS method as described above.

### Epifluorescence microscopy

The fluorescein-labelled oligonucleotide-patterned surfaces were visualized using a Zeiss Axiovert 200 inverted microscope with epifluorescence illumination fitted with a Zeiss Filterset 09. All samples were placed face down on a drop of phosphate buffer (10 mM phosphate, 0.3 M NaCl, pH 7.0) on a glass slide towards Epiplan Neofluar 10× or 20× objective lenses.

## RESULTS AND DISCUSSION

### Overview: formation of oligonucleotide patterns on silicon

Our previously reported two-step method for covalent attachment of oligonucleotides onto crystalline silicon surfaces in patterns has been exploited for attachment of DNA sequences to the silicon surface (Figure 1) (4). The subsequent coupling of the *N*-hydroxysuccinimide ester terminated surface with an amino-modified oligonucleotides [Series A (see Table 1)] in an aqueous solution, led to its covalent attachment of the single-stranded DNA (ssDNA) sequences (See Figure 2a for the schematic showing the composition of the linker and spacer). In this study, DNA oligonucleotides are attached to silicon surfaces via the *linker* with a chain of 18 atoms and a *spacer* made of oligomers of one, two and six hexaethylene glycol phosphate diester groups with monomers each with a chain of 20 atoms in the monomer. These chains provided combined linker and spacer lengths with 18, 38, 58 and 138 atoms long, covering a full range of chain lengths; Southern *et al*. suggested that chains of 30–60 atoms between surfaces and DNA sequences are optimal for hybridization (17), and thus the chain lengths chosen for the studies reported here cover this range.

The patterns of attached DNA sequences were revealed by epifluorescence microscopy after hybridization with FAM-labelled complementary DNA sequences [A′-com (see Table 1)], and a fluorescence signal of >95% of the desired pattern was achieved. Shown in Figure 3 are typical epifluorescent images of the samples (after incubation and washing with buffer) with the 5′-end FAM-labelled complementary sequence (A′-com), a sequence containing a mis-matched thymine residue in the sequence (A′1-mis) and a sequence that is not complementary to the probe sequence (A′-non). There is limited to no levels of fluorescence revealed in the samples treated with the sequence containing a mis-matched thymine residue in the sequence (A′1-mis) and the sequence that is not complementary to the probe sequence (A′-non). The level of fluorescence detected for the sample prepared with the sequence $A\text{-}EG_{91}$ and hybridized with the complementary sequence A′-com is far lower than for any of the other samples hybridized with A′-com.

### Quantification of density of surface-immobilized probe

Quantification of the surface-immobilized probe DNA density is necessary, as this has been demonstrated to influence the efficiency for hybridization (11). The quantification of the probe density of DNA conjugated onto surfaces has been achieved using radio-labelled oligonucleotides (14,17,39,40). Radioactive-labelled oligonucleotides have a short shelf-life, are hazardous and are only accessible to research laboratories with the appropriate infrastructure. Although an approach using alkaline phosphatase digestion has been reported for the quantitative evaluation of the surface coverage of oligonucleotides

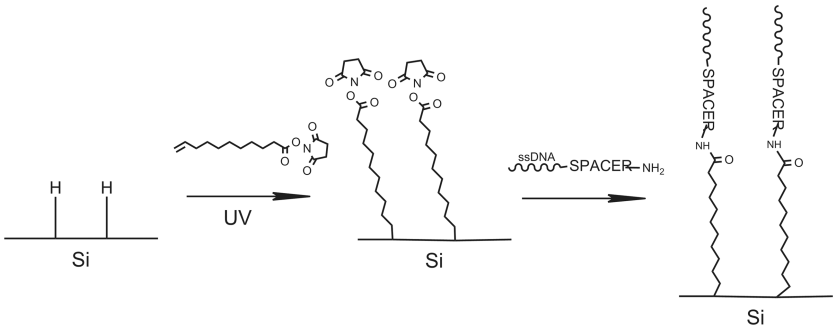


**Figure 1.** Schematic showing the steps for immobilization of oligonucleotides onto silicon surfaces.

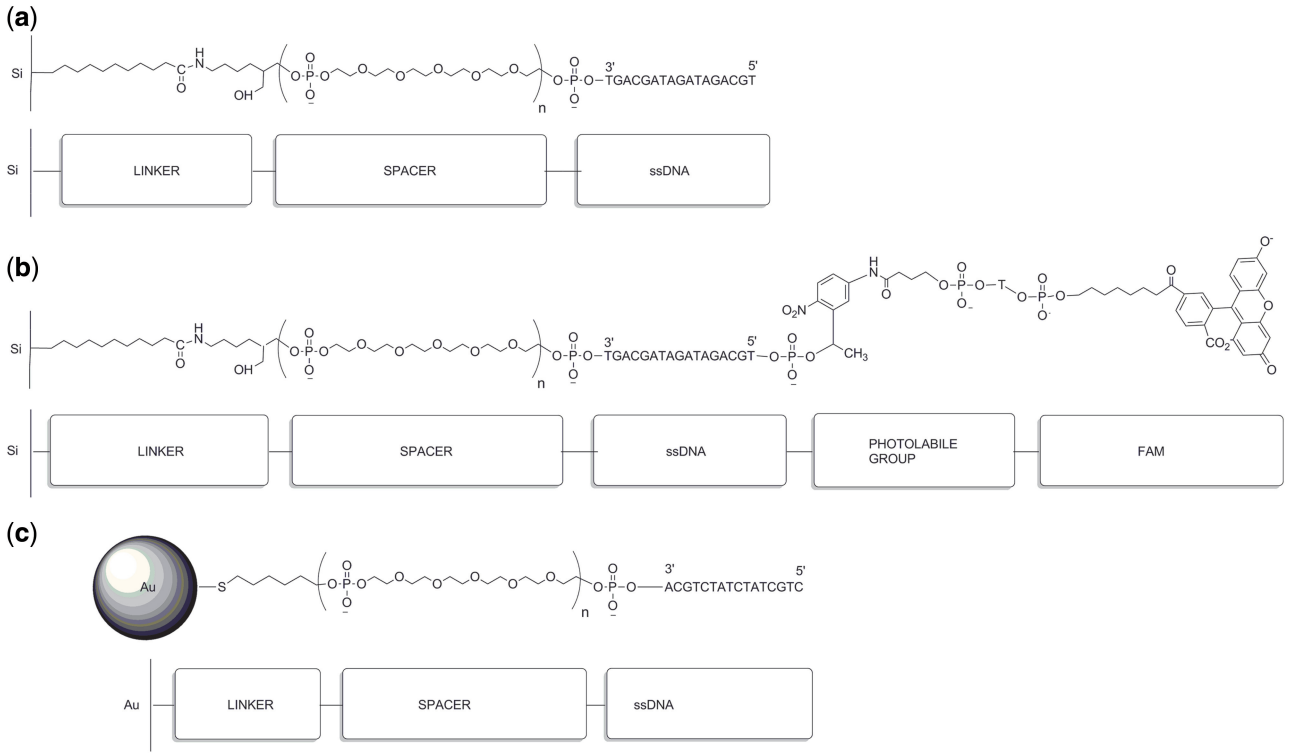


**Figure 2.** Schematic showing the chemical groups used for conjugation to surfaces. (**a**) The DNA oligonucleotide linkage to the silicon surface. The figure shows the undecylamide 'linker' to the silicon surface attached via a hexyl chain (termed the 'linker') to the hexaethene glycol phosphate diester chain oligomer (termed the 'spacer'), where $n = 0$, 1, 2, 6. The spacer is conjugated to the 3′-end of the DNA oligonucleotide. (**b**) The DNA oligonucleotide conjugation used to establish the immobilization density at the silicon surface. The surface attachment is the same as in (a) but the oligonucleotide is 5′-end labelled with a photolabile group [1-(2-nitrophenyl)-propane-1,3-phosphate diester] attached to FAM via a thymine residue. (**c**) The DNA oligonucleotide linkage to the gold nanoparticle (10 nm). The gold nanoparticle (10 nm) linked via a thiol linkage to a hexyl chain and then to the spacer, where $n = 0$, 6 (for E-HEG$_0$-GNP and E-HEG$_6$-GNP, respectively). The spacer is linked to the 3′-end of the DNA oligonucleotide.

at relatively low densities (~$10^9$ oligonucleotides\cm$^2$) (41), polyethylene glycol is well known to interact with proteins (42). An alternative approach to establish the immobilized density of DNA oligonucleotides with ethylene glycol oligomer spacers was required. Here we have developed a simpler safer fluorescence-based technique for the determination of the surface-attachment density of DNA oligonucleotides based on the work of Ju *et al*. (37). In short, a photolabile linker based on a 2-nitrobenzyl group is attached between the 5′-end of the oligonucleotide and the FAM label, to the 3′-end of the oligonucleotide is the 'spacer' group that is linked to a hexyl amino group used to attach to the *N*-hydroxysuccinimide ester surface (Figure 2b). The nitrobenzyl group offers a highly efficient photocleavable group and is easily incorporated into DNA oligonucleotides during DNA synthesis by the use of commercially available phosphoramidite derivatives (43). Here the DNA sequence (Series A, Table 1) is attached to the silicon surface via attachment to the *N*-hydroxysuccinimide ester surface and only the FAM released by UV illumination. The photoreaction, as reported, results in FAM-photolabile group release leaving behind the DNA oligonucleotide still attached to the surface (37). The FAM-containing

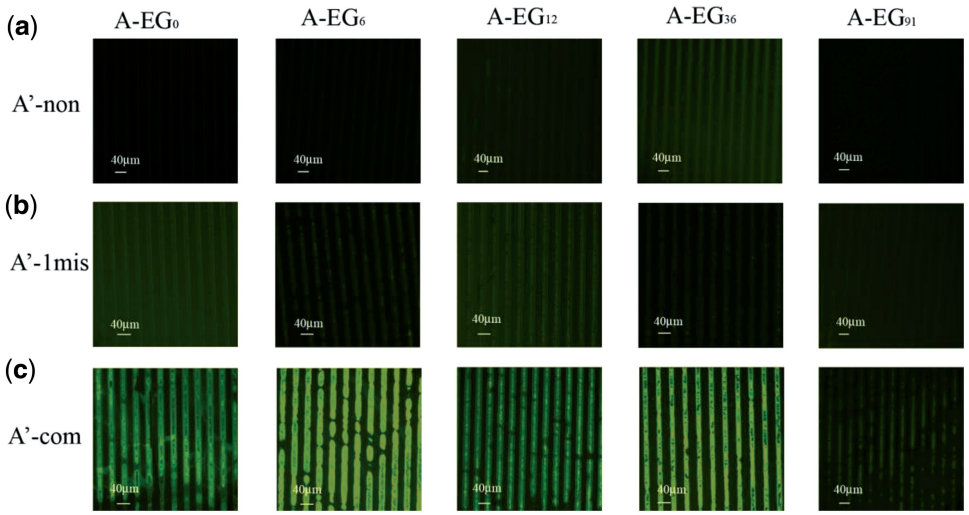


**Figure 3.** Epifluorescent images of the patterns of A-series of oligonucleotides (A-HEG$_0$, A-HEG$_1$, A-HEG$_2$, A-HEG$_6$ and A-EG$_{91}$) on silicon surfaces after hybridization with fluorescein-labelled (**a**) non-complementary sequences (A′-non), (**b**) sequences containing a single mismatch (A′-1mis) and (**c**) complementary sequence (A′-com). The sequences used are identified in Table 1.

molecules are collected and the DNA immobilized density established as detailed in the 'Materials and Methods' section.

A study was carried out by illumination of each of the B-series oligonucleotides in aqueous solution using the band pass filtered UV irradiation ($375 \pm 25$ nm) of a HgXe lamp at a range of illumination intensities from 10 to 50 mW/cm$^2$, and a range of illumination periods from 10 to 120 min. The UV absorption peak of DNA (260 nm) and the fluorescence quantum yield of FAM ($\lambda_{exc} = 488$ nm) were monitored to establish the optimal photolysis conditions to release the FAM without damage to the DNA oligonucleotide. No obvious change was observed at a UV absorbance of 260 nm after photolysis under any of the conditions studied, indicating a negligible quantity of DNA photolysis products, such as thymine dimers. A decrease in the fluorescence quantum yield of the solution was observed after photolysis. This variability in the reduction in fluorescence yield with filtered UV illumination, for example, repeat individual experiments of oligonucleotide B-HEG$_6$ solutions (at $1 \times 10^{-8}$ M after photolysis at 20∼25 mW/cm$^2$ for 30 min) showed a decrease from initial values by $53 \pm 1\%$ for three samples. Standardization curves prepared from a series of FAM-photolabile group-oligonucleotide solutions of known concentration after the photolysis showed a linear relationship between oligonucleotide concentration and fluorescence intensity. These results demonstrate that the quantification of immobilized oligonucleotides on silicon surfaces can be achieved by reference to a standard curve of the same type of oligonucleotide under the same photolysis conditions. The photolysis yield, as determined by HPLC, approached 100% at illumination intensities >25 mW/cm$^2$ and >30 min exposure. Therefore, an illumination intensity of ∼28 mW/cm$^2$ for 30 min was used for the photolysis of immobilized oligonucleotides on silicon surfaces, and for the calibration standards.

Shown in Table 2 is the immobilized density of B-series oligonucleotides covalently attached on silicon surfaces. High densities of $5.4–9.6 \times 10^{12}$ strands/cm$^2$ for oligonucleotides with and without hexaethylene glycol phosphate diester oligomers have been achieved.

### The effect of spacer on the surface-attached DNA oligonucleotides on the hybridization density for fluorescently labelled and gold-nanoparticle-labelled oligonucleotides

#### *Fluorophore-labelled DNA oligonucleotide*

The immobilized densities for the DNA sequences A-HEG$_0$, A-HEG$_1$, A-HEG$_2$ and A-HEG$_6$ on silicon are listed in Table 2. The oligonucleotide used is C-com, which is the 3′-FAM end-labelled complementary DNA sequence to provide consistency with the 3′-GNP end-labelled complementary DNA sequence used (see studies below). There is a small variation in the immobilized density for the sequences A-HEG$_0$, A-HEG$_1$, A-HEG$_2$ and A-HEG$_6$ on silicon as well as a small difference in the hybridization density with C-com. To take into account the minor difference in the immobilized density, the hybridization efficiency was calculated (Table 2). For all cases, a high efficiency of hybridization was obtained, of almost full occupancy of the immobilized complementary sequences. In short, one DNA hybrid is formed on average for every ∼20–40 nm$^2$, which is almost at the density of the immobilized complementary sequence. Some of the earlier reports have shown that the hybridization yield increases where the hexaethylene glycol phosphate diester chain length increases (10,11). For the system studied here, with both a surface linker and a spacer, the length of the hexaethylene glycol phosphate diester oligomer spacer has an effect, if minor, on the hybridization efficiency for oligonucleotide C-com. The hybridization efficiency for the surface-immobilized sequences A-HEG$_1$, A-HEG$_2$ and A-HEG$_6$ is slightly higher than with surface-immobilized A-HEG$_0$ (Table 2). Although

**Table 2.** Densities of the immobilized oligonucleotides on silicon surfaces and the complementary ssDNA strands hybridized onto them

| Immobilized DNA | Number of atoms between DNA and silicon surface | Immobilized density number/cm$^2$ ($\times 10^{12}$) | Hybridization density number/cm$^2$ ($\times 10^{12}$) | Hybridization efficiency[a] |
|---|---|---|---|---|
| A-HEG$_0$ | 18 | 5.4 ± 0.8 | 2.3 ± 0.3 | 42% |
| A-HEG$_1$ | 38 | 9.6 ± 2.1 | 5.9 ± 0.7 | 62% |
| A-HEG$_2$ | 58 | 7.3 ± 1.9 | 4.8 ± 0.9 | 67% |
| A-HEG$_6$ | 138 | 5.4 ± 0.7 | 3.8 ± 0.7 | 70% |

[a]Hybridization efficiency, determined from the immobilized density versus the hybridization density.

A-HEG$_0$ has the lowest surface-immobilized density, there is a relatively small increase in the hybridization efficiency with length of hexaethylene glycol phosphate diester spacer from A-HEG$_1$, A-HEG$_2$ to A-HEG$_6$.

### *GNP of 1.4 nm conjugated with a single complementary strand (HEG$_0$-GNP 1.4 nm)*

The hybridization of immobilized oligonucleotides on silicon surfaces with DNA–GNP conjugates was investigated. Two types of DNA–GNP conjugates were used: a 1.4 nm GNP conjugated with a single complementary strand (HEG$_0$-GNP 1.4 nm) and a 10-nm gold nanoparticle labelled with multiple complementary strands (HEG$_0$-GNP 10 nm), described below.

A new method was developed for the determination of the number of DNA–GNPs hybridized to surface-attached complementary sequences. In brief, DNA–GNP samples were hybridized with the DNA-functionalized silicon surfaces, washed and then released by heating the substrate at 90°C in an aqueous solution. The collected solution containing the released DNA–GNP conjugates from the DNA sequences attached to surface were evaluated by ICP–MS following the method described in Pitcairn *et al*. (38) (see 'Materials and Methods' section).

Figure 4 contains plots of the hybridization densities of DNA–GNP conjugates (HEG$_0$-GNP 1.4 nm), and these can be compared directly on the same plot with the hybridization densities of the fluorescently labelled DNA (C-com) onto immobilized A-HEG$_0$, A-HEG$_1$, A-HEG$_2$ and A-HEG$_6$ oligonucleotide patterns on silicon. There is no significant variation in the hybridization density for 1.4 nm DNA–GNP conjugates as a function of the spacer length (A-HEG$_0$, A-HEG$_1$, A-HEG$_2$ and A-HEG$_6$) of the sequence attached to the silicon surface. The hybridization density of 1.4 nm DNA–GNP conjugates is approximately four times lower than for fluorescently labelled DNA (C-com), but this still represents a hybridization efficiency of between 10 and 20%—which is good, providing a hybridization density of $\sim 1 \times 10^{12}$ DNA–GNP (1.4 nm)/cm$^2$—or one complementary sequence per ~100 nm$^2$. The lack of variation in the hybridization density suggests that hexaethylene glycol phosphate diester spacers between the immobilized oligonucleotides and the silicon surface have a minor effect on their hybridization with HEG$_0$-GNP (1.4 nm) conjugates.

### *GNP of 10 nm conjugated with multiple complementary strands (HEG$_0$-GNP 10 nm)*

The 3′-thiol end-labelled DNA oligonucleotide (Table 1, E-HEG) was conjugated to 10 nm gold nanoparticles; the chemical structure of the linkage is shown in Figure 2c. So far a direct method for the quantification of thiol-terminated oligonucleotides coupled onto GNPs has not been reported. The feed ratio of thiol-terminated oligonucleotides to GNPs used in the synthesis does not provide the number of strands per DNA–GNP because the yield of attachment is influenced by surface adsorption and the equilibrium, oligonucleotide length, nucleotide bases and even washing steps during the preparation (13,28,44). Existing methods for the determination of surface coverage of oligonucleotides on GNPs are fluorescence based (13). However, accurate data for this existing approach is dependent on the successful removal of the GNPs from the fluorescent labels, so a new method where the elemental composition is quantified has been developed here.

Phosphorus exists stoichiometrically in DNA and can be quantified using ICP–OES with an accuracy of ~1% (45). Quantification of the amount of phosphorus by ICP–OES and gold by ICP–MS in the same sample provides a new approach to deduce the ratio of phosphorus to gold and hence the number of oligonucleotides to GNPs. This has been applied in this study. In all cases, the actual ratio of oligonucleotides bound to GNPs is less than the feed ratio. The average surface coverage of HEG$_0$ oligonucleotides on GNPs at a feed ratio of 200 is 124 ± 8 strands per nanoparticle (corresponding to 66 ± 4 pmol/cm$^2$, $3.9 \times 10^{13}$ strands/cm$^2$). This coverage is consistent to that reported for DNA–GNP conjugates prepared in a similar manner (42 pmol/cm$^2$) (13).

Figure 4 contains a plot of the hybridization densities of HEG$_0$-GNP 10 nm, in comparison with those of the ssDNA (C-com) and HEG$_0$-GNP 1.4 nm onto immobilized A-HEG$_0$, A-HEG$_1$, A-HEG$_2$ and A-HEG$_6$ oligonucleotide patterns on silicon. The hybridization density of the HEG$_0$-GNP 10 nm with the A-HEG$_0$, A-HEG$_1$, A-HEG$_2$ and A-HEG$_6$ oligonucleotides attached on the silicon are not significantly different and is $\sim 3 \times 10^{10}$ hybrids/cm$^2$ or ~1 hybrid per ~3000 nm$^2$. In fact, the hybridization density of A-HEG$_0$-GNP 10 nm conjugates is lower by a factor of 30 as compared with the A-HEG$_0$-GNP 1.4 nm conjugates and yet again is not determined simply by the length of the spacer for the oligonucleotide attached to a planar silicon surface. Thus, the size of the GNP in the DNA–GNP conjugates appears to be an important factor affecting hybridization at surfaces and the yield of hybridization. An increased DNA–GNP conjugate dimension would occupy a higher exclusive cross-section area, and cause the hybridization density to be

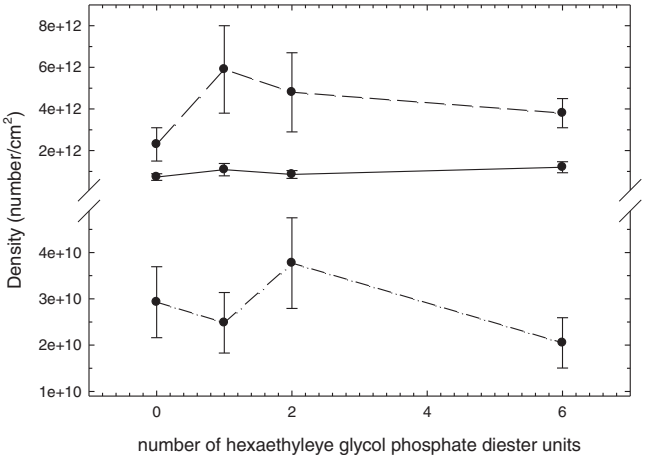


**Figure 4.** Plot of the hybridization density of fluorescently labelled DNA (C-com), DNA–GNP conjugates (E-HEG$_0$-Au 1.4 nm and E-HEG$_0$-Au 10 nm) onto oligonucleotide patterns (A-HEG$_0$, A-HEG$_1$, A-HEG$_2$ and A-HEG$_6$) on silicon surfaces versus number of hexaethylene glycol phosphate diester oligomers. Hybridization density of the DNA-modified silicon surfaces after hybridization with the FAM-labelled complementary stands (dash line), GNP (1.4 nm)–ssDNA conjugates (solid line) and GNP (10 nm)–DNA conjugates (dash-dot line). Error bars shown are standard error of the mean.

lower than for the A-HEG$_0$-GNP 1.4 nm or C-com. In solution, the hydrodynamic radius of a short DNA chain of <20 bases has been determined to be 1 nm (46) and 8.7 for a 10-nm GNP labelled with multiple 12 bp DNA oligonucleotides prepared in a similar manner (16). Using published data (46), the approximate ratio of exclusive cross-section areas between an HEG$_0$-GNP 10 nm conjugate and an ssDNA (A-HEG$_0$, 17 base) strand is estimated to be ~75. This difference, however, is too small to account for the observed difference in hybridization density. This suggests that the reduced flexibility of a DNA strand after attachment to the 10 nm GNP and steric hindrance between neighbouring strands on the DNA–GNP 10 nm conjugates are the major determinants impacting on the hybridization efficiency. Additional factors that may influence the hybridization efficiency could include electrostatic factors resulting from the surface charge of the GNP or the high density of DNA attached; however, under the saline buffer conditions used, these effects are anticipated to be minor.

### *Ten nanometre GNP conjugated with multiple complementary strands containing a hexaethylene glycol phosphate diester oligomer (HEG$_6$-GNP 10 nm)*

A hexaethylene glycol phosphate diester oligmer spacer group between the gold nanoparticle (10 nm) surface and the attached single-stranded oligonucleotides was tested to establish the effect on the yield of hybridization. The ratio of oligonucleotides per nanoparticle was determined by ICP–OES and ICP–MS methods, as detailed above. At a feed ratio of 200 oligonucleotides per GNP, 144 ± 3 strands of E-HEG$_6$ oligonucleotides per nanoparticle were determined, resulting in a higher packing density (76 ± 1 pmol/cm$^2$, $4.6 \times 10^{13}$ strands/cm$^2$) in comparison with the oligonucleotides E-HEG$_0$ (124 ± 8 strands per nanoparticle). Of note, a previous report indicates that the insertion of 20-dA or 20-dT spacers leads to a lower surface coverage of oligonucleotides on GNPs (13). The small improvement in the surface coverage of GNPs with the oligonucleotide E-HEG$_6$ as compared with DNA with 20-dA or 20-dT spacers could be a result of two factors: (i) a transition from an amorphous coil to a brush-like state occurring as the packing density of oligonucleotides increase, which is a well known scenario for polyethylene glycol layers of higher molecular weight (Mw > 1000) (47,48); and (ii) the cross-section of an EG unit in its idealized helical form is only 0.21 nm$^2$ (49) in comparison with that of ssDNA at 0.9 nm$^2$ (the cross-section of ssDNA is 1.07 nm). So, more DNA strands containing hexaethylene glycol phosphate diester oligomer spacers could be accommodated onto the 10-nm nanoparticle surface as a result of spatial reasons.

The hybridization density of the E-HEG$_6$-GNP 10 nm conjugates onto the immobilized complementary strands A-HEG$_0$ (Figure 5a) is $1.26 \pm 0.24 \times 10^{11}$ particles/cm$^2$, which is more than four times higher than that of the E-HEG$_0$-GNP (10 nm) onto immobilized complementary strands A-HEG$_0$ (Figure 5b) ($3.1 \pm 0.8 \times 10^{10}$ particles/cm$^2$), showing a significant enhancement for hybridization of E-HEG$_6$-GNP 10 nm due to the presence of hexaethylene glycol phosphate diester oligomer spacer on the GNP surface. The hybridization density of E-HEG$_0$-GNP 10 nm onto silicon surface functionalized with A-HEG$_6$ (Figure 5c) is $2.1 \pm 0.5 \times 10^{10}$ particles/cm$^2$. The hybridization density of E-HEG$_6$-GNP 10 nm conjugates onto the immobilized complementary strands A-HEG$_0$ (Figure 5a) is six times higher than for E-HEG$_0$-GNP 10 nm conjugates onto A-HEG$_6$ (Figure 5c). These results suggest that the presence of the spacer of oligomeric hexaethylene glycol phosphate diester has the biggest impact when present on the 10-nm GNP–DNA conjugate. Incorporating the hexaethylene glycol phosphate diester oligomer spacer on the GNP surface will result in the following: (i) a greater distance of the DNA from the GNP surface and thus higher accessibility of the conjugated DNA strands; and (ii) a greater cross-sectional area of the DNA–GNP conjugate as a result of the increased spacer size. Thus, on collision with the DNA functionalized silicon surface, the E-HEG$_6$-GNP will occupy a higher coverage (by up to ~50 nm diameter) as compared with E-HEG$_0$-GNP (by up to ~23 nm diameter) (see Figure 5). DNA hybridization occurs via a two-step process: (i) DNA nucleation, followed by (ii) rapid zippering to yield the duplex (35). It is thus possible that there are both a higher probability of nucleation due to increased flexibility of the linker-spacer chain of E-HEG$_6$-GNP and coverage of the underlying silicon-DNA surface on collision (Figure 5).

Given the cross-sectional area of the DNA–GNP (10 nm) conjugates, taking into account the size of the attached DNA oligonucleotides and spacers, the density of hybridized DNA–GNP conjugates is high and is typically more than one DNA–GNP (10 nm) per ~3000 nm$^2$. Thus the method represents an efficient approach for the self-assembly of GNPs on silicon surfaces. It is anticipated

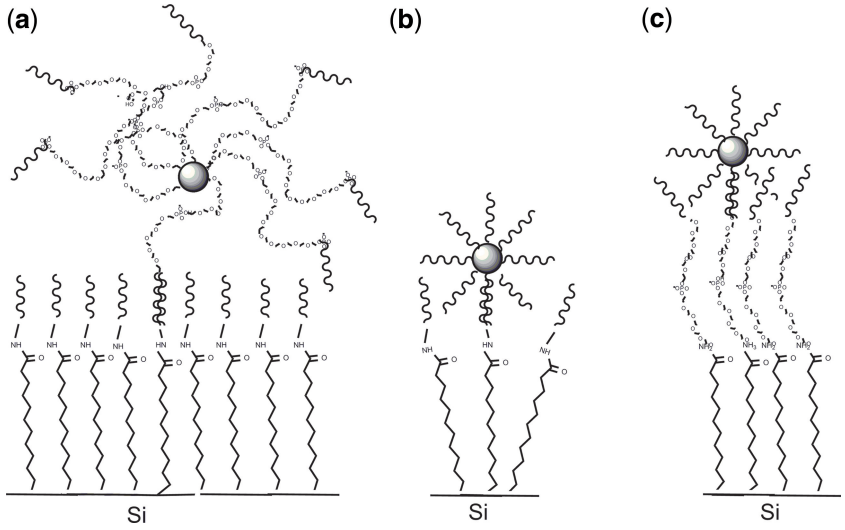


**Figure 5.** Schematic showing silicon surfaces functionalized with DNA oligonucleotides with (**a**) no spacer linkage (A-$HEG_0$) and hybridized with DNA with a hexaethylene glycol phosphate diester oligomer chain Spacer linked to a gold nanoparticle (10 nm) (E-$HEG_6$-GNP 10 nm). The figure is not drawn to scale, the GNP is 10 nm diameter, the DNA strand (shown by the wavy line) is ~5 nm long and the spacer $HEG_6$ is ~15 nm long (fully extended). (**b**) No spacer linkage (A-$HEG_0$) and hybridized with DNA with no spacer, but linked to a gold nanoparticle (10 nm) (E-$HEG_0$-GNP 10 nm). The linker between the GNP and DNA is ~1 nm long and the linker between the silicon and DNA is 2.4 nm. (**c**) a hexaethylene glycol phosphate diester oligomer chain spacer (A-$HEG_6$) hybridized with DNA sequences linked to gold nanoparticles (10 nm diameter) without a spacer (E-$HEG_0$-GNP 10 nm). The figure is not drawn to scale, the linker attached to the silicon surface is ~2.4 nm and the spacer, $HEG_6$ is ~15 nm long (fully extended).

that other nanoparticles and surfaces could be self-assembled in a similar manner.

## CONCLUSIONS

Our approach in performing this study is to develop quantitative approaches to provide an accurate evaluation of (i) the immobilization density of DNA on the surface of silicon and on the surface of gold nanoparticles and to then evaluate (ii) the hybridization efficiency of surface-attached DNA as a function of the attachment chemistry. For our case, we have developed DNA-attachment chemistry to provide high hybridization efficiencies for fluorophore-labelled DNA with the surface-attached DNA. The silicon surfaces, as studied, provide efficient hybridization of fluorophore-labelled DNA hybridization with efficiencies of between 42 and 70%. Even with the high hybridization efficiencies, there is a small trend showing improved efficiencies as a function of the spacer length. In contrast, tuning the spacer length for the DNA oligonucleotide attached to the silicon surface does not have a major effect on the yield of DNA–GNP hybridization, whether for DNA–GNP (1.4 nm) or DNA–GNP (10 nm). The hybridization efficiencies of DNA–GNP were proportional to the nanoparticle size. The DNA–GNP (1.4 nm) hybridization efficiencies were only marginally less efficient than the fluorophore-labelled DNA hybridization efficiency, but independent of the spacer size for the DNA attached to the surface. The density for hybridization for the E-$HEG_0$-DNA (10 nm), even taking into account the cross-section of the hybrid, was poor. The incorporation of a hexaethylene glycol phosphate diester oligomer between the gold nanoparticle and the DNA oligonucleotide (E-$HEG_{36}$-DNA) with the A-$HEG_0$-DNA attached to the silicon surface provided a 6-fold increase in the hybridization density as compared with E-$HEG_0$-DNA with the A-$HEG_{36}$-DNA attached to the silicon surface. These results suggest that the attachment linker and spacer length of the DNA attached to the gold nanoparticle of 10 nm has a more significant impact than the attachment linker and spacer length of the DNA attached to the silicon surface. This is most likely a function the DNA molecule attached on the gold nanoparticle via a hexaethylene glycol phosphate diester linker being more free to diffuse around on the silicon surface during collision with the DNA functionalized silicon surface.

The DNA conjugation method reported here provides a simple and reliable way to provide controllable interfaces between silicon surfaces and gold nanoparticles. Although the size of the gold nanoparticle has a major impact on the hybridization yield at the surface, the approach reported here provides high yields of hybridization of fluorophore and 1.4-nm gold nanoparticle-labelled DNA with complementary sequences on a silicon surface. Application of the method is likely to offer potential for the creation of bioanalytical tools and nanobioelectronic structure fabrication.

## FUNDING

We are grateful for the financial support of the Biotechnology and Biological Sciences Research Council (References E16611 and 51/E18926) and the Royal Society (Biomolecule Patterns on Silicon). Funding for open access charge: A partial waiver of fees is gratefully acknowledged, the remaining fees are funded from personal research funds.

*Conflict of interest statement*. None declared.

## REFERENCES


1. Patole,S.N., Pike,A.R., Connolly,B.A., Horrocks,B.R. and Houlton,A. (2003) STM study of DNA films synthesized on Si(111) surfaces. *Langmuir*, **19**, 5457–5463.
2. Strother,T., Hamers,R.J. and Smith,L.M. (2000) Covalent attachment of oligodeoxyribonucleotides to amine-modified Si (001) surfaces. *Nucleic Acids Res.*, **28**, 3535–3541.
3. Yin,H.B., Brown,T., Greef,R., Mailis,S., Eason,R.W., Wilkinson,J.S. and Melvin,T. (2004) In: Faupel,M.D.M.P. (ed.), *Proc. SPIE Biophotonics New Frontier: From Genome to Proteome*, Vol. 5461, pp. 1–8.
4. Yin,H.B., Brown,T., Greef,R., Wilkinson,J.S. and Melvin,T. (2004) Chemical modification and micropatterning of Si(100) with oligonucleotides. *Microelectron. Eng.*, **73–74**, 830–836.
5. Yin,H.B., Brown,T., Wilkinson,J.S., Eason,R.W. and Melvin,T. (2004) Submicron patterning of DNA oligonucleotides on silicon. *Nucleic Acids Res.*, **32**, e118.
6. Fritzsche,W. and Taton,T.A. (2003) Metal nanoparticles as labels for heterogeneous, chip-based DNA detection. *Nanotechnology*, **14**, R63–R73.
7. Kohler,J.M., Csaki,A., Reichert,J., Moller,R., Straube,W. and Fritzsche,W. (2001) Selective labeling of oligonucleotide monolayers by metallic nanobeads for fast optical readout of DNA-chips. *Sens. Actuators B Chem.*, **76**, 166–172.
8. Niemeyer,C.M. and Ceyhan,B. (2001) DNA-directed functionalization of colloidal gold with proteins. *Angew. Chem. Int. Ed. Engl.*, **40**, 3685–3688.
9. Storhoff,J.J. and Mirkin,C.A. (1999) Programmed materials synthesis with DNA. *Chem. Rev.*, **99**, 1849–1862.
10. Peterson,A.W., Heaton,R.J. and Georgiadis,R. (2000) Kinetic control of hybridization in surface immobilized DNA monolayer films. *J. Am. Chem. Soc.*, **122**, 7837–7838.
11. Peterson,A.W., Heaton,R.J. and Georgiadis,R.M. (2001) The effect of surface probe density on DNA hybridization. *Nucleic Acids Res.*, **29**, 5163–5168.
12. Watterson,J.H., Piunno,P.A.E., Wust,C.C. and Krull,U.J. (2000) Effects of oligonucleotide immobilization density on selectivity of quantitative transduction of hybridization of immobilized DNA. *Langmuir*, **16**, 4984–4992.
13. Demers,L.M., Mirkin,C.A., Mucic,R.C., Reynolds,R.A., Letsinger,R.L., Elghanian,R. and Viswanadham,G. (2000) A fluorescence-based method for determining the surface coverage and hybridization efficiency of thiol-capped oligonucleotides bound to gold thin films and nanoparticles. *Anal. Chem.*, **72**, 5535–5541.
14. Guo,Z., Guilfoyle,R.A., Thiel,A.J., Wang,R.F. and Smith,L.M. (1994) Direct fluorescence analysis of genetic polymorphisms by hybridization with oligonucleotide arrays on glass supports. *Nucleic Acids Res.*, **22**, 5456–5465.
15. Parak,W.J., Pellegrino,T., Micheel,C.M., Gerion,D., Williams,S.C. and Alivisatos,A.P. (2003) Conformation of oligonucleotides attached to gold nanocrystals probed by gel electrophoresis. *Nano Lett.*, **3**, 33–36.
16. Xu,J. and Craig,S.L. (2005) Thermodynamics of DNA hybridization on gold nanoparticles. *J. Am. Chem. Soc.*, **127**, 13227–13231.
17. Shchepinov,M.S., CaseGreen,S.C. and Southern,E.M. (1997) Steric factors influencing hybridisation of nucleic acids to oligonucleotide arrays. *Nucleic Acids Res.*, **25**, 1155–1161.
18. Vainrub,A. and Pettitt,B.M. (2003) Sensitive quantitative nucleic acid detection using oligonucleotide microarrays. *J. Am. Chem. Soc.*, **125**, 7798–7799.
19. Vainrub,A. and Pettitt,B.M. (2003) Surface electrostatic effects in oligonucleotide microarrays: control and optimization of binding thermodynamics. *Biopolymers*, **68**, 265–270.
20. Gong,P. and Levicky,R. (2008) DNA surface hybridization regimes. *Proc. Natl Acad. Sci. USA*, **105**, 5301–5306.
21. Halperin,A., Buhot,A. and Zhulina,E.B. (2006) Hybridization at a surface: the role of spacers in DNA microarrays. *Langmuir*, **22**, 11290–11304.
22. Halperin,A., Buhot,A. and Zhulina,E.B. (2005) Brush effects on DNA chips: thermodynamics, kinetics, and design guidelines. *Biophys. J.*, **89**, 796–811.
23. Cha,T.W., Boiadjiev,V., Lozano,J., Yang,H. and Zhu,X.Y. (2002) Immobilization of oligonucleotides on poly(ethylene glycol) brush-coated Si surfaces. *Anal. Biochem.*, **311**, 27–32.
24. Lasseter,T.L., Clare,B.H., Abbott,N.L. and Hamers,R.J. (2004) Covalently modified silicon and diamond surfaces: resistance to nonspecific protein adsorption and optimization for biosensing. *J. Am. Chem. Soc.*, **126**, 10220–10221.
25. Peeters,S., Stakenborg,T., Reekmans,G., Laureyn,W., Lagae,L., Van Aerschot,A. and Van Ranst,M. (2008) Impact of spacers on the hybridization efficiency of mixed self-assembled DNA/alkanethiol films. *Biosens. Bioelectron.*, **24**, 72–77.
26. Li,S., Li,X., Zhang,J., Zhang,Y., Han,J. and Jiang,L. (2010) Quantitative investigation of the influence of gold nanoparticles on the dynamics of DNA hybridization using a programmed multi-channel quartz crystal microbalance system. *Colloids Surfaces Physicochem. Eng. Aspects*, **364**, 158–162.
27. Chen,C., Wang,W., Ge,J. and Zhao,X.S. (2009) Kinetics and thermodynamics of DNA hybridization on gold nanoparticles. *Nucleic Acids Res.*, **37**, 3756–3765.
28. Storhoff,J.J., Elghanian,R., Mucic,R.C., Mirkin,C.A. and Letsinger,R.L. (1998) One-pot colorimetric differentiation of polynucleotides with single base imperfections using gold nanoparticle probes. *J. Am. Chem. Soc.*, **120**, 1959–1964.
29. Fong,K.E. and Yung,L.-Y.L. (2012) Analysis of metallic nanoparticle-DNA assembly formation in bulk solution via localized surface plasmon resonance shift. *RSC Adv.*, **2**, 5154–5163.
30. Barchanski,A., Hashimoto,N., Petersen,S., Sajti,C.L. and Barcikowski,S. (2012) Impact of spacer and strand length on oligonucleotide conjugation to the surface of ligand-free laser-generated gold nanoparticles. *Bioconjugate Chem.*, **23**, 908–915.
31. Han,M.S., Lytton-Jean,A.K.R., Oh,B.K., Heo,J. and Mirkin,C.A. (2006) Colorimetric screening of DNA-binding molecules with gold nanoparticle probes. *Angew. Chem. Int. Ed.*, **45**, 1807–1810.
32. Liu,J.W. and Lu,Y. (2003) A colorimetric lead biosensor using DNAzyme-directed assembly of gold nanoparticles. *J. Am. Chem. Soc.*, **125**, 6642–6643.
33. Dreyfus,R., Leunissen,M.E., Sha,R., Tkachenko,A., Seeman,N.C., Pine,D.J. and Chaikin,P.M. (2010) Aggregation-disaggregation transition of DNA-coated colloids: experiments and theory. *Phys. Rev. E Stat. Nonlin. Soft Matter Phys.*, **81(4 Pt 1)**, 041404.
34. Leunissen,M.E., Dreyfus,R., Sha,R., Seeman,N.C. and Chaikin,P.M. (2010) Quantitative study of the association thermodynamics and kinetics of DNA-coated particles for different functionalization schemes. *J. Am. Chem. Soc.*, **132**, 1903–1913.
35. Oh,J.-H. and Lee,J.-S. (2011) Designed hybridization properties of DNA-gold nanoparticle conjugates for the ultraselective detection of a single-base mutation in the breast cancer gene BRCA1. *Anal. Chem.*, **83**, 7364–7370.
36. Dyadyusha,L., Yin,H., Jaiswal,S., Brown,T., Baumberg,J.J., Booy,F.P. and Melvin,T. (2005) Quenching of CdSe quantum dot emission, a new approach for biosensing. *Chem. Commun.*, **2005**, 3201–3203.
37. Bai,X.P., Li,Z.M., Jockusch,S., Turro,N.J. and Ju,J.Y. (2003) Photocleavage of a 2-nitrobenzyl linker bridging a fluorophore to the 5′ end of DNA. *Proc. Natl Acad. Sci. USA*, **100**, 409–413.
38. Pitcairn,I.K., Warwick,P.E., Milton,J.A. and Teagle,D.A.H. (2006) Method for ultra-low-level analysis of gold in rocks. *Anal. Chem.*, **78**, 1290–1295.
39. Chrisey,L.A., Oferrall,C.E., Spargo,B.J., Dulcey,C.S. and Calvert,J.M. (1996) Fabrication of patterned DNA surfaces. *Nucleic Acids Res.*, **24**, 3040–3047.
40. Moiseev,L., Unlu,M.S., Swan,A.K., Goldberg,B.B. and Cantor,C.R. (2006) DNA conformation on surfaces measured by fluorescence self-interference. *Proc. Natl Acad. Sci. USA*, **103**, 2623–2628.
41. Pal,S., Kim,M.J. and Song,J.M. (2008) Quantitation of surface coverage of oligonucleotides bound to chip surfaces: a fluorescence-based approach using alkaline phosphatase digestion. *Lab. Chip.*, **8**, 1332–1341.

42. Fahie-Wilson,M. and Halsall,D. (2008) Polyethylene glycol precipitation: proceed with care. *Ann. Clin. Biochem.*, **45**, 233–235.
43. McMinn,D.L. and Greenberg,M.M. (1996) Novel solid phase synthesis supports for the preparation of oligonucleotides containing S3′-alkyl amines. *Tetrahedron*, **52**, 3827–3840.
44. Stillman,B.A. and Tonkinson,J.L. (2001) Expression microarray hybridization kinetics depend on length of the immobilized DNA but are independent of immobilization substrate. *Anal. Biochem.*, **295**, 149–157.
45. Yang,I., Han,M.S., Yim,Y.H., Hwang,E. and Park,S.R. (2004) A strategy for establishing accurate quantitation standards of oligonucleotides: quantitation of phosphorus of DNA phosphodiester bonds using inductively coupled plasma-optical emission spectroscopy. *Anal. Biochem.*, **335**, 150–161.
46. Eimer,W. and Pecora,R. (1991) Rotational and translational diffusion of short rodlike molecules in soluton - oligonucleotides. *J. Chem. Phys.*, **94**, 2324–2329.
47. Fick,J., Steitz,R., Leiner,V., Tokumitsu,S., Himmelhaus,M. and Grunze,M. (2004) Swelling behavior of self-assembled monolayers of alkanethiol-terminated poly(ethylene glycol): a neutron reflectometry study. *Langmuir*, **20**, 3848–3853.
48. Tokumitsu,S., Liebich,A., Herrwerth,S., Eck,W., Himmelhaus,M. and Grunze,M. (2002) Grafting of alkanethiol-terminated poly(ethylene glycol) on gold. *Langmuir*, **18**, 8862–8870.
49. Harder,P., Grunze,M., Dahint,R., Whitesides,G.M. and Laibinis,P.E. (1998) Molecular conformation in oligo(ethylene glycol)-terminated self-assembled monolayers on gold and silver surfaces determines their ability to resist protein adsorption. *J. Phys. Chem. B*, **102**, 426–436.